Applied Thermal Engineering 108 (2016) 1418–1428

Contents lists available at ScienceDirect

Applied Thermal Engineering

journal homepage: www.elsevier.com/locate/apthermeng

Research Paper

Thermo-Electric Energy Storage involving CO_2 transcritical cycles and ground heat storage

Fadhel Ayachi [a], Nicolas Tauveron [a,*], Thomas Tartière [b], Stéphane Colasson [a], Denis Nguyen [c]

[a] CEA, LITEN – DTBH/SBRT/LS2T, 17 rue des Martyrs, Grenoble 38054, France
[b] Enertime, 1 rue du Moulin des Bruyères, Courbevoie 92400, France
[c] BRGM Languedoc-Roussillon, 1039 rue de Pinville, 34000 Montpellier, France

HIGHLIGHTS

- With ideal hypotheses roundtrip efficiencies can be up to 50%.
- With ideal hypotheses roundtrip efficiencies reach 66% with the most complex cycle.
- More realistic roundtrip efficiencies were evaluated between 42.5 and 55.5%.

ARTICLE INFO

Article history:
Received 16 March 2016
Revised 15 June 2016
Accepted 10 July 2016
Available online 11 July 2016

Keywords:
Storage
CO_2
Transcritical
Ground
Heat-pump
Rankine

ABSTRACT

Multi-megawatt Thermo-Electric Energy Storage based on thermodynamic cycles is a promising alternative to PSH (Pumped-Storage Hydroelectricity) and CAES (Compressed Air Energy Storage) systems. The size and cost of the heat storage are the main drawbacks of this technology but using the ground as a heat reservoir could be an interesting and cheap solution. In that context, the aim of this work is (i) to assess the performance of a geothermal electricity storage concept based on CO_2 transcritical cycles and ground heat exchanger, and (ii) to carry out the preliminary design of the whole system. This later includes a heat pump transcritical cycle as the charging process and a transcritical Rankine cycle of 1–10 MW_{el} as the discharging process.

A steady-state thermodynamic model is performed and several options, including heat regeneration, two-phase turbine and multi-stage design, are investigated. In addition, a one-dimensional model of the ground exchanger is performed and coupled to the thermodynamic model to optimize the number of wells for the ground heat storage.

The results show a strong dependency between the charging and discharging processes and indicate how the use of heat regeneration in both processes could be advantageous. The results also measure the difference in performance between the basic and the advanced designs.

1. Introduction

Organic Rankine Cycles (ORC) have been used in a wide range of applications (including geothermal, biomass, solar power plants, waste heat recovery from industrial processes and combustion engines, ocean thermal energy conversion) and a wide range of power outputs from a few kilowatts to tens of megawatts. The possibility to use ORC to produce electricity from heat that has been previously stored as a large-scale electricity storage technology remains more confidential but has been the subject of recent studies [1].

As it is well-known, the massive integration of intermittent renewable energy production generates new challenges for the supervision and regulation of electric grids. The use of flexible but carbon-intensive technologies such as gas turbines has been the main solution in order to ensure the balance between demand and supply, maintaining grid frequency and power quality. However, large-scale electricity storage is a promising alternative with a much lower environmental impact. In addition, it would enable a decentralized access to electricity and lower the dependency on fossil fuels. If storage is still expensive today, it could become increasingly viable as the price of carbon rises.

Several technologies exist or are under development for large-scale energy storage. Pumped-Storage Hydroelectricity (PSH) is the most common one and covers a power range varying from a

* Corresponding author.
E-mail address: nicolas.tauveron@cea.fr (N. Tauveron).

http://dx.doi.org/10.1016/j.applthermaleng.2016.07.063
1359-4311/

Nomenclature

Latin letters

A	column area (m^2)
h	specific enthalpy (J/kg)
$\dot{m}$	overall mass flow rate (g/s)
$\dot{m}_{series}$	mass flow rate per series (g/s)
N	nunmber of columns per series
Nb	total column number
Nu	Nusselt number
P	pressure (Pa) or (bar)
P_H	cycle high pressure (Pa) or (bar)
P_L	cycle low pressure (Pa) or (bar)
Pr	Prandtl number
PR	Turbine pressure ratio
$\dot{Q}$	heat flux (W)
Re	Reynolds number
s	specific entropy (J/kg K)
T	temperature (K) or (°C)
U	heat transfer coefficient (W/m^2 K)
$\dot{W}$	power (W)
$\dot{W}_{el}$	electrical power (W)

Greek letters

$\delta\dot{Q}_{cold}$	system asymmetry (W)
ΔP	pressure drop (Pa) or (bar)
$\Delta T_{\min}$	minimum temperature difference between reservoir and fluid (K)
η	efficiency
η_{th}	thermal efficiency
η_{sys}	roundtrip efficiency of the storage system
ρ	density (kg/m^3)

Subscripts

c	compressor
cold	cold reservoir
g	generator
hot	hot reservoir
m	motor
p	pump
reg	heat regenerator
s	isentropic
t	turbine
tp	two-phase turbine
w	wall

Acronyms

COP	Coefficient Of Performance
CFD	Computational Fluid Dynamics
ORC	Organic Rankine Cycle
TEES	Thermo-Electric Energy Storage

few hundred of megawatts to a few gigawatts. It accounts for more than 99% of the worldwide bulk storage capacity, representing around 140 GW over 380 locations [1]. Reported storage efficiencies are typically between 70% and 85%. Despite having a long lifetime and being the most cost-effective energy storage technology, these systems have a low energy density and require the construction of large water reservoirs, leading to a high environmental impact. In addition, the most suitable locations have already been used in developed countries. Other possibilities would be to include pre-existing dams or the ocean, as in the 30 MW Yanbaru project in Japan [2].

At a lower power range varying from a few tens to a few hundreds of megawatts, Compressed-Air Energy Storage (CAES) is at an advanced stage of development and accounts only 2 power plants until now: a 290 MW plant in Huntorf, Germany (1978) [3], and a 110 MW plant in McIntosh, USA (1991) [4]. Reported roundtrip efficiencies are around 50% and the capital cost of CAES power plants is competitive with PSH. A much higher efficiencies up to 70% could be achieved by Advanced Adiabatic CAES (AA-CAES) [4–6] as the second generation technology which is still at an early stage of development. Such as PSH, CAES and AA-CAES systems require specific sites and cannot be installed everywhere.

Thermo-electric energy storage (TEES) is a promising alternative to existing technologies that covers widespread and large-scale electricity storage. It couples thermodynamic cycles to independent reservoirs and is generally free from geological and geographical constraints. During periods of excess electricity generation, a vapour compression heat pump consumes electricity and transfers heat between a low-temperature heat source and a higher temperature heat sink. The temperature difference between the heat sink and the heat source can be maintained for several hours, until a power cycle is used to discharge the system and generate electricity during peak consumption hours.

Mercangöz et al. [7] gave references of Thermo-Electric Energy Storage studies as old as 1924 and described the general concept of this technology, based on two-way conversion of electricity to and from heat. They noted that the main challenges of TEES are to closely match the working fluid operation to the heat source and heat sink profiles, and to find an optimum between roundtrip efficiency and capital cost. The authors have analysed a TEES system with CO_2 transcritical cycles, hot water and ice tanks as storage reservoirs. The ABB Corporate Research Center [8,9] described a way to store electricity using two hot water tanks, an ice tank and CO_2 transcritical cycles. For similar systems, Morandin et al. [10,11] defined a design methodology based on pinch analysis and calculated a 60% maximum roundtrip efficiency for a base case scenario with turbomachinery efficiencies given by manufacturers.

Sensible heat storage with hot water tanks is often considered, since water has high thermal capacity, cheaply available and environmental-friendly. Latent heat storages based on phase-change materials (PCMs) have also been widely investigated. The heat sink of the system can be either the ambient or ice. This second option ensures a constant low-pressure for the process that is favorable to turbomachines. A mixture of salt and water can be used to adjust the heat sink temperature between 0 °C and −21.2 °C (corresponding to the eutectic point with 23.3% NaCl in water by mass) [10].

Different working fluids can be considered for the thermodynamic cycles. Desrues et al. [12] presented a TEES process based on Argon in forward and backward closed Brayton cycles. Henchoz et al. [13] analysed the combination of solar thermal energy with TEES based on Ammonia cycles. Kim et al. [14] reviewed current TEES systems and showed that using CO_2 transcritical cycles instead of Argon Brayton cycles leads to a higher roundtrip efficiency even if the required temperature difference between the heat storages is much smaller. They also proposed an isothermal energy storage system based on CO_2 transcritical cycles and liquid piston compressors/expanders.

Carbon dioxide is a natural refrigerant with many advantages. It is a low-cost fluid that is non-toxic, non-flammable, chemically

stable, and cheaply available. In addition, the high fluid density of supercritical CO_2 leads to very compact systems. Many studies have been published to evaluate the potential of supercritical CO_2 as working fluid in power cycles and heat pumps [15,16]. Cayer et al. carried out an analysis [17] and an optimization [18] of CO_2 transcritical cycle with a low-temperature heat source. More recently, the use of CO_2 for multi-megawatt power cycles has reached a commercial step with the American company Echogen [19]. In parallel, underground thermal energy storage appears to be an attractive solution [20].

The purpose of this article is to introduce a new concept of Thermo Electric Energy Storage process for large scale electric applications, based on CO_2 transcritical cycles and ground heat storage. The association of such cycles and ground storage constitutes the originality of the project. The conceptual design of such TEES system is addressed here only from a thermodynamic point of view and economic analysis are left for future work.

2. Problem definition

The investigated Thermo-Electric Energy Storage system is a geothermal storage concept that includes:

i. a hot reservoir made of ground heat exchangers organized in a serial-parallel layout and set up in a superficial bedrock (unfractured crystalline dry rock)
ii. a cold reservoir using a phase-change material that could be ice ($T_{cold} \leqslant 0$ °C) or other material ($T_{cold} > 0$ °C)
iii. two thermodynamic cycles as a charging process and a discharging process both using carbon dioxide as a working fluid.

The basic overviews of these two processes are given respectively by Figs. 1 and 2. All the components of each process are considered as open systems in steady state condition.

During off-hours, the charging process consists of a transcritical heat pump cycle characterized by 6 main steps: the working fluid leaves the cold reservoir heat exchanger as a saturated vapour at $T_1 = T_{cold} - \Delta T_{min}$ and is internally superheated ($1 \rightarrow 2$) through a regenerator, before being adiabatically compressed ($2 \rightarrow 3$) into a mechanical compressor with an isentropic efficiency $\eta_{s,c}$. At the compressor outlet, the fluid at $T_3 = (T_{hot})_{max} + \Delta T_{min}$ and supercritical high pressure $P_3 = P_H$ is first cooled through the hot reservoir exchanger ($3 \rightarrow 4$) releasing heat to the ground, then cooled further through the regenerator ($4 \rightarrow 5$) releasing heat to the low pressure vapour. The fluid at a liquid state passes into an expansion valve ($5 \rightarrow 6$) to reach the subcritical low pressure P_L and is finally evaporated through the cold reservoir exchanger ($6 \rightarrow 1$).

For given storage temperatures T_{cold} and $(T_{hot})_{max}$ and a given hot pressure P_H, the thermodynamic states can be obtained from the energy balances of the system components:

$$(h_1 - h_2) + (h_4 - h_5) = 0 \quad (1)$$

$$\dot{W}_c + \dot{m}(h_2 - h_3) = 0 \quad (2)$$

$$\dot{Q}_{hot} + \dot{m}(h_3 - h_4) = 0 \quad (3)$$

$$h_5 - h_6 = 0 \quad (4)$$

$$\dot{Q}_{cold} + \dot{m}(h_6 - h_1) = 0 \quad (5)$$

h_i (J/kg K) and $\dot{m}$ (kg/s) being respectively the specific enthalpy at state i and the mass flow rate relating to the charging cycle. $\dot{W}_c(W) = \dot{m}(h_{3s} - h_2)/\eta_{s,c} > 0$, $\dot{Q}_{hot}(W) < 0$ and $\dot{Q}_{cold}(W) > 0$ are respectively the compressor power, the heat flux transferred to the hot reservoir and the heat flux transferred from the cold reservoir.

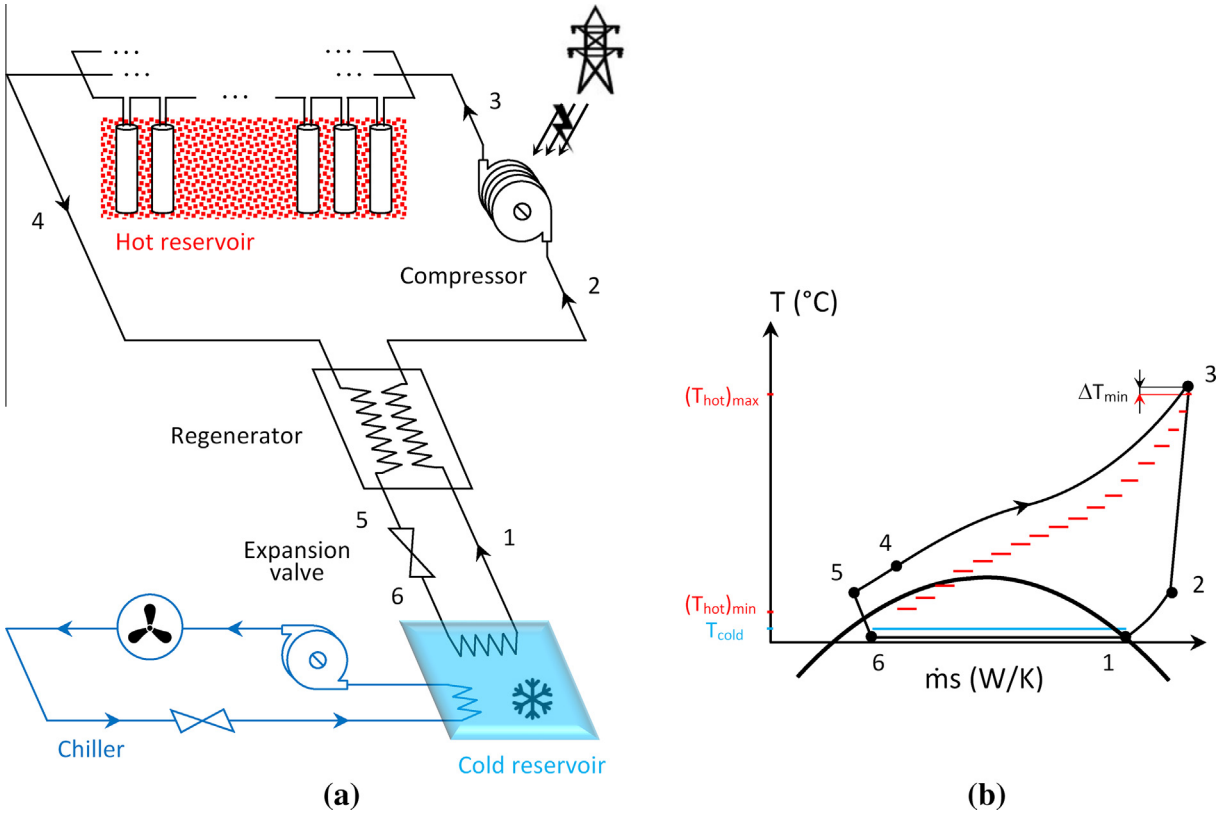

Fig. 1. Charging process: (a) process layout, (b) (T, ṁs) diagram.

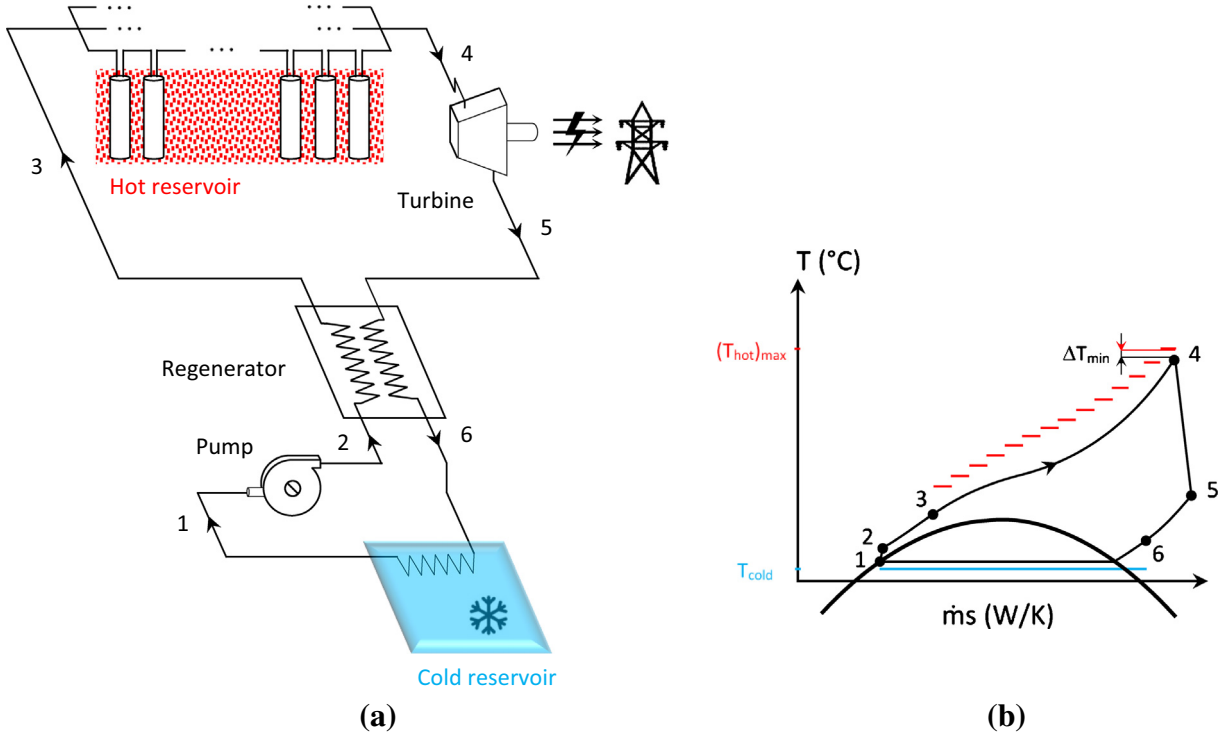

Fig. 2. Discharging process: (a) process layout, (b) (T, ṁs) diagram.

By adding Eqs. (1)–(5), it appears the energy balance of the charging cycle:

$$\dot{W}_c + \dot{Q}_{hot} + \dot{Q}_{cold} = 0 \tag{6}$$

During peak-hours, the discharging process consists of a transcritical Rankine cycle characterized by 6 main steps: the working fluid leaves the cold reservoir heat exchanger as a saturated liquid at $T_1' = T_{cold} + \Delta T_{min}$ and is adiabatically compressed ($1 \rightarrow 2$) into a feed pump with an isentropic efficiency $\eta_{s,p}$. At the outlet of the pump, the fluid at a supercritical high pressure $P_2' = P_H'$ is first preheated through the regenerator ($2 \rightarrow 3$), then heated further through the hot reservoir exchanger ($3 \rightarrow 4$) destocking heat from the ground. At the entrance of the turbine, the fluid at $T_4' = (T_{hot})_{max} - \Delta T_{min}$ is adiabatically expanded ($4 \rightarrow 5$) to the subcritical low pressure P_L' delivering a mechanical work with an isentropic efficiency $\eta_{s,t}$. Finally, the fluid is internally cooled through the regenerator ($5 \rightarrow 6$) before being condensed through the cold reservoir exchanger ($6 \rightarrow 1$).

The reservoir temperatures T_{cold} and $(T_{hot})_{max}$ and the high pressure $P_H' \approx P_H$ being known, the thermodynamic states can be obtained from the energy balances of the system components:

$$\dot{W}_p' + \dot{m}'(h_1' - h_2') = 0 \tag{7}$$
$$(h_2' - h_3') + (h_5' - h_6') = 0 \tag{8}$$
$$\dot{Q}_{hot}' + \dot{m}'(h_3' - h_4') = 0 \tag{9}$$
$$\dot{W}_t' + \dot{m}'(h_4' - h_5') = 0 \tag{10}$$
$$\dot{Q}_{cold}' + \dot{m}'(h_6' - h_1') = 0 \tag{11}$$

h_i' (J/kg K) and $\dot{m}'$ (kg/s) being respectively the specific enthalpy at state i and the mass flow rate relating to the discharging cycle. $\dot{W}_p'(W) = \dot{m}'(h_{2s}' - h_1')/\eta_{s,p} > 0$, $\dot{W}_t'(W) = \dot{m}'(h_{5s}' - h_4')\eta_{s,t} < 0$, $\dot{Q}_{hot}'(W) > 0$ and $\dot{Q}_{cold}'(W) < 0$ are respectively the pump power, the turbine power, the heat flux transferred from the hot reservoir and the heat flux transferred to the cold reservoir.

By adding Eqs. (7)–(11), it appears the energy balance of the discharging cycle:

$$\dot{W}_p' + \dot{Q}_{hot}' + \dot{W}_t' + \dot{Q}_{cold}' = 0 \tag{12}$$

By specifying the net power output of the discharging cycle $\dot{W}_{el}' = \eta_g(\dot{W}_t' + \dot{W}_p')$ and by assuming similar charging and discharging times, $\dot{Q}_{hot}' \cong -\dot{Q}_{hot}$. This gives the mass flow rates $\dot{m}$ and $\dot{m}'$ and then the net power input of the charging cycle $\dot{W}_{el} = \dot{W}_c/\eta_m$.

Furthermore, by adding Eqs. (6) and (12) and since $\dot{Q}_{hot}' = -\dot{Q}_{hot}$, it follows that:

$$\dot{W}_c + \dot{Q}_{cold} + \dot{W}_p' + \dot{W}_t' + \dot{Q}_{cold}' = 0 \tag{13}$$

Eq. (13) shows that there is an asymmetry between the two processes which can be expressed as an additional need of cooling:

$$\delta\dot{Q}_{cold} = \dot{Q}_{cold} + \dot{Q}_{cold}' = -(\dot{W}_c + \dot{W}_p' + \dot{W}_t') < 0 \tag{14}$$

This additional need of cooling can be provided by an auxiliary CO_2 chiller that processes independently and simultaneously with the charging cycle (Fig. 1a). The electrical consumption of the chiller $\dot{W}_{el}''(W)$ as expressed by Eq. (15) is calculated using a single stage chiller model with a condensing temperature at 20 °C.

$$\dot{W}_{el}'' = \frac{-\delta\dot{Q}_{cold}}{COP} \tag{15}$$

On the other hand, the low diffusivity of the ground ensures the heterogeneity of the temperature therein (Figs. 1b and 2b), which seems to be favorable to maintain the cycles uniforms at their nominal conditions over a long period of time. Assuming similar charging and discharging times, the roundtrip efficiency of the whole system can be defined as:

$$\eta_{sys} = \frac{\dot{W}_{el}'}{\dot{W}_{el} + \dot{W}_{el}''} \tag{16}$$

Table 1
Input parameters.

Storage	
Hot storage max temperature $(T_{hot})_{max}$	130 °C
Cold storage temperature T_{cold}	Variable
Min temperature difference between reservoir and fluid ΔT_{min}	Variable
Charging cycle	
Compressor isentropic efficiency $\eta_{s,c}$	0.85
Motor efficiency η_m	0.98
$(T_4)_{min}$	30 °C
Regenerator pinch	5 K
Regenerator pressure drop	[0–5 bar]
Discharging cycle	
Net power output $\dot{W}'_{el}$	[1–10 MW_{el}]
Pump isentropic efficiency $\eta_{s,p}$	0.80
Turbine isentropic efficiency $\eta_{s,t}$	0.90
Generator efficiency η_g	0.98
Regenerator pinch	5 K
Regenerator pressure drop	[0–5 bar]
Chiller	
Compressor isentropic efficiency	0.85
Motor efficiency	0.98
Condensing temperature	20 °C
Evaporating temperature	Same as for discharge cycle

It is worth noting that the system performance as expressed above also relies on the stabilization of the ground temperature at the start of each process i.e. $T_{hot} = (T_{hot})_{min}$ at the start of the charging process and $T_{hot} = (T_{hot})_{max}$ at the start of the discharging process. This implies the achievement of a certain control during the shutdown sequence of each process in order to set and stabilize the ground temperature at the convenient value for the start of each following process.

Thereby, this steady-state analysis can be useful as a first approach for the assessment of the system performance especially at nominal conditions. This could be sufficient as a comparative tool for the selection of the system design (non-regenerative, regenerative, single-stage, multi-stage) before coupling dynamically the charging and discharging processes to the ground properties.

The thermodynamic model is implemented through the Engineering Equation Solver (EES) software [21]. The model input parameters are reported in Table 1. The component efficiencies including the generator and the rotary machines are fixed at commonly used values at nominal conditions [22–30].

3. System design analysis

From the thermodynamic model described above, it is possible to carry out a parametric study of the whole system. As the aim of this section is to perform a comparative design analysis basing on the maximum reachable efficiencies, the quasi-limit case (ΔT_{min} = 1 K) is then first considered and the pressure losses within the hot reservoir exchanger are preliminarily neglected. The component efficiencies including the rotary devices are fixed at nominal values (Table 1). Once these settings are given, two cycle independent variables, namely the cold storage temperature T_{cold} and the high pressure P_H are sufficient for describing the whole system.

The performance map given by Fig. 3 illustrates the iso-efficiencies according to the couple (T_{cold}, P_H) and with respect to the system design. The map indicates that the roundtrip efficiency of a non-regenerative system reaches an optimal value of 45% at potentially high pressures. This could lead to more expensive devices. The implementation of heat regeneration in the discharging cycle leads to comparable performances with the advantage of lower operating pressures. Moreover, the implementation of heat regeneration in both charging and discharging cycles leads to an optimal roundtrip efficiency slightly higher than 50%. It is worth noting that the lower the cold temperature T_{cold} is, the lower the high pressure P_H is.

Figs. 4a and b represent the entropy diagrams of respectively an optimal non-regenerative system and an optimal regenerative system. By comparing the two diagrams, it can be seen that the double regeneration reduces the system high pressures P_H and P'_H and

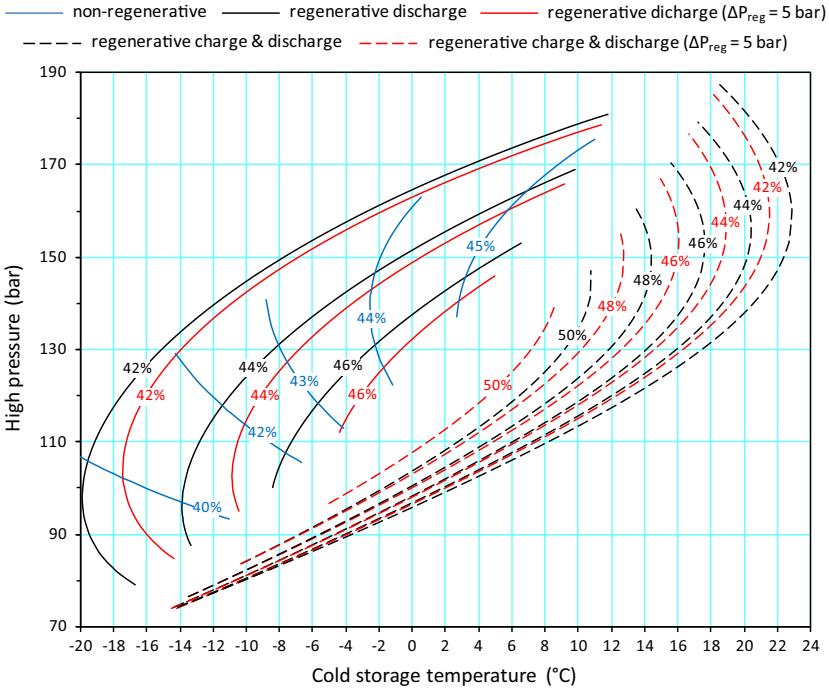

Fig. 3. Performance map of the basic storage system (ΔT_{min} = 1 K).

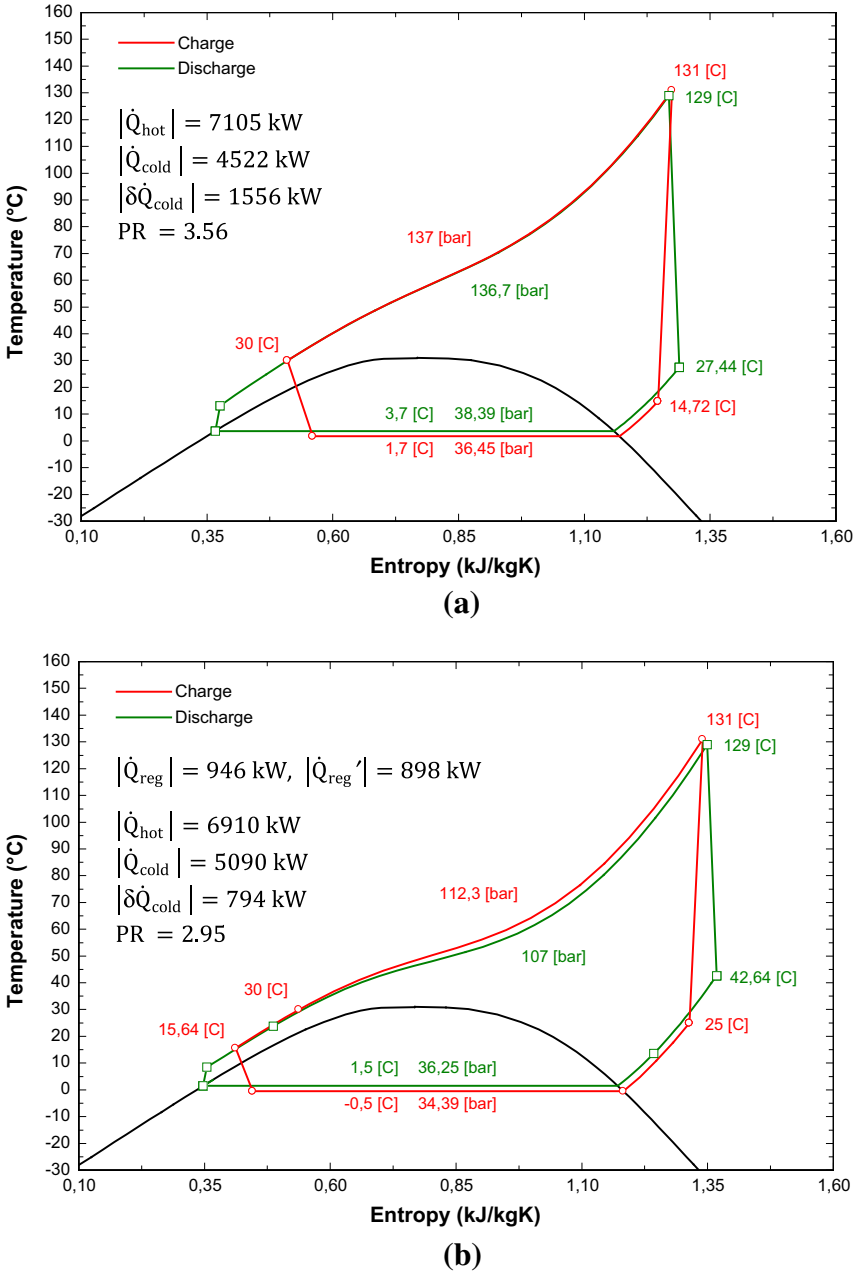

Fig. 4. Entropy diagram (ΔT_{min} = 1 K, $\dot{W}'_{el}$ = 1 MW_{el}). (a) non-regenerative basic system (η_{sys} = 45%), (b) regenerative basic system (η_{sys} = 51%).

reduces in more the turbine pressure ratio PR, the heat flux transferred to the hot reservoir $\dot{Q}_{hot}$ and the additional supply of cooling because of the asymmetry existence $\delta\dot{Q}_{cold}$. Thereby, the double regeneration appears very attractive to meet high efficiency and low investment cost.

The improvement of the roundtrip efficiency could be made by complicating the system design. Therefore, it would be interesting to thermodynamically assess the performance of:

- a storage system including a two-phase turbine in the charging cycle. In this case, the two-phase turbine substitutes the expansion valve in the evolution (5 → 6) and the net power input is then reduced by the two-phase turbine generation
- a storage system including a two-stage discharging cycle. In this case, Fig. 5 shows that the heat transfer is made via two pressure levels and the thermoelectric conversion is done via two expansion stages
- a storage system including a two-phase turbine in the charging cycle and a two-stage discharging cycle.

Figs. 6a, b and c respectively illustrate the improvement in efficiency given by the aforementioned designs. The two first ones lead to comparable improvements e.g. the addition of a two-phase turbine in the charging cycle or a second stage in the discharging cycle lead to a gain in the range of [9–14%] by considering the regenerative system. Notice that the higher (T_{cold}, P_H) are, the bigger is the gain in efficiency. Furthermore, the addition of both two-phase turbine in the charging cycle and second stage in the discharging cycle lead to a promising gain range of [17–29%] depending on the couple (T_{cold}, P_H) i.e. an efficiency range of [60–66%]. Fig. 7 gives the entropy diagram of this advanced design and highlights the specific effect of the heat regeneration in the discharging cycle as a consequence of the second stage addition.

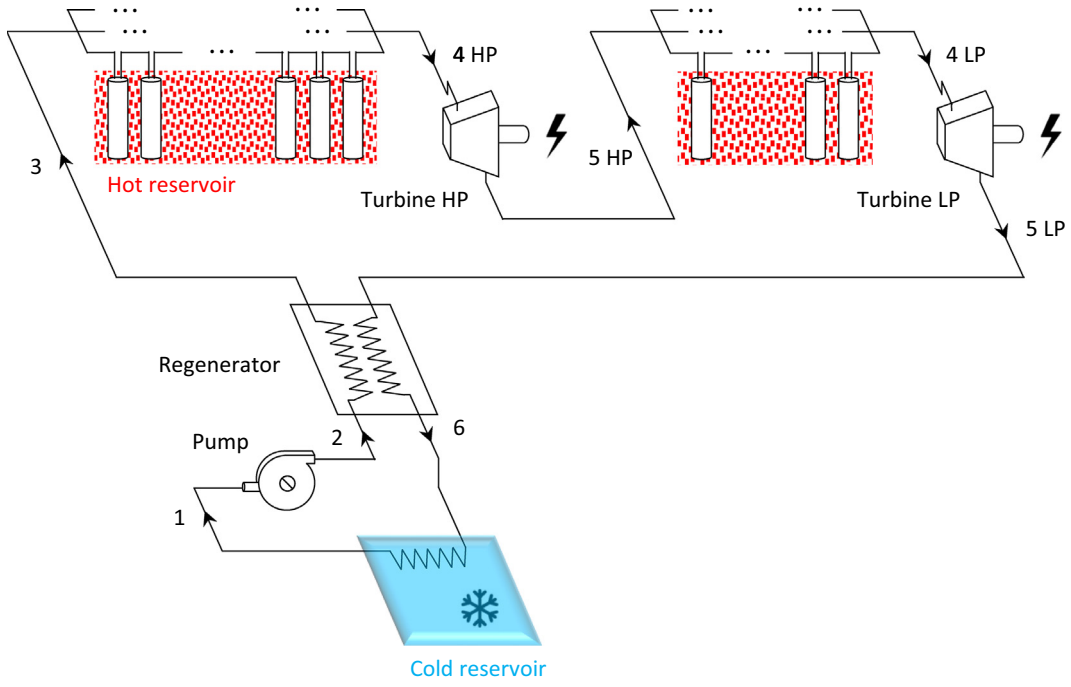

Fig. 5. Two-stage discharging process: process layout.

It is obvious that these high performances would be lowered by the impact of the pressure losses mainly through the high-pressure heat exchanger. In the following section, the heat transfer simulation will enable to estimate the head losses in that component and adjust the system parameters, in particular the minimum temperature difference ΔT_{min}.

4. Heat transfer modelling and exchanger preliminary design

The hot reservoir heat exchanger is made of multiple vertical columns having the same geometry. Series of columns are set in parallel lines as shown in Figs. 1 and 2.

It is worth noting that the quasi-limit case (ΔT_{min} = 1 K), analysed in the previous section, could be constrained on one hand by the exchange area and then the number of drillings and columns to implement and on the other hand by the pressure drop that it generates. Thus, it is particularly important to consider these constraints in the thermodynamic study of the system, which would need to process to a preliminary design of the hot reservoir heat exchanger according to the minimum temperature difference ΔT_{min} setting.

In this regard, the one-dimensional modelling is a simple and fast tool requiring few computing resources. This makes easy the coupling of the hot reservoir heat exchanger model to the thermodynamic model of the storage system. While it provides limited accuracy, the one-dimensional model of the heat exchanger could be useful to determine the suitable ΔT_{min} setting and particularly helpful to indicate how optimizing the geometric configuration of the unitary column. The heat exchanger design would be conveniently refined thereafter by using advanced tools such as the CFD simulation.

4.1. Model description

Fig. 8 gives the conceptual scheme of the 1D discretization applied to a series of columns. The fluid at supercritical pressure is injected at the bottom of each column through a central tube and then flows up to an annular exit, exchanging heat with the surrounding rock. We consider each column as a homogeneous rod thermally insulated from the other columns. We assume that there is no radial or vertical temperature gradient within each column, and therefore the temperature within one column is homogeneous. The central injection tube is assumed adiabatic by considering a thin insulation coating. The column specifications are reported in Table 2.

The preliminary design of the heat exchanger is performed through EES on the basis of the nominal conditions of the discharging process. This preliminary design could also be valid for the charging process when adapting the initial ground temperature $(T_{hot})_{min}$ (Fig. 1b).

For a given ΔT_{min}, the boundary conditions of the hot reservoir heat exchanger are:

$\{T[1,1] = T'_3, \quad T[N,K+1] = T'_4, \quad T_{hot}[N] = (T_{hot})_{max}, T_{hot}[1] \gtrsim (T'_3 + \Delta T_{min})\}$. For a given power output, the overall mass flow rate $\dot{m}'$ (kg/s) and then the overall heat flux $\dot{Q}'_{hot} = -\dot{Q}_{hot}$ are distributed according to the number of series:

$$\dot{Q}'_{hot} = \dot{Q}'_{series} \times \frac{Nb_{columns}}{N}, \quad \dot{m}' = \dot{m}'_{series} \times \frac{Nb_{columns}}{N} \tag{17}$$

On the other hand, the heat flux transferred through one series verifies the discretization concept:

$$\dot{Q}'_{series} = \sum_{i=1}^{N}\sum_{j=1}^{K}\dot{Q}[i,j] \tag{18}$$

where

$$\begin{aligned}\dot{Q}[i,j] &= \frac{A}{K}U[i,j]LMTD[i,j] \\ &= \dot{m}'_{series}(h[i,j+1] - h[i,j])\end{aligned} \tag{19}$$

For each elementary segment, the log mean temperature difference is given by:

$$LMTD[i,j] = \frac{\Delta T[i,j] - \Delta T[i,j+1]}{\ln\left(\frac{\Delta T[i,j]}{\Delta T[i,j+1]}\right)} \tag{20}$$

with

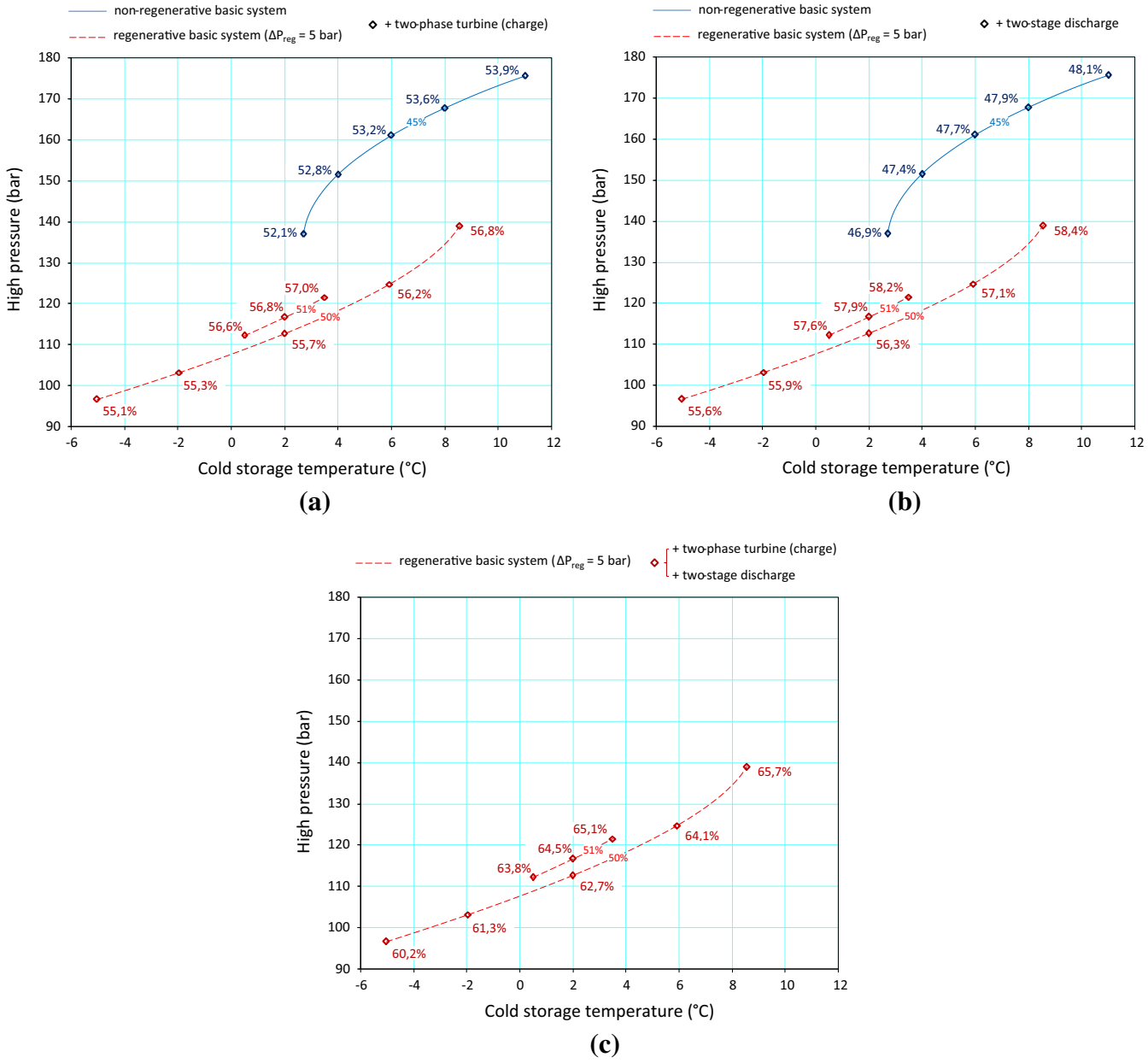

Fig. 6. Efficiency improvement (ΔT_{min} = 1 K) given by: (a) two-phase turbine (η_{tp} = 0.75), (b) two-stage discharging process, (c) advanced design.

$$\Delta T[i,j] = T[i,j] - T_{hot}[i] \tag{21}$$

The model includes the calculation of both the regular pressure losses occurred within the central tube and the annular and the singular pressure losses due to the elbows, the sudden narrowing at the top of the column and the sudden enlargement at the bottom of the column:

$$\begin{cases} P[i+1,1] = P[i,K+1] - (P_{tube}[i+1] + \sum \Delta P_{sing}[i+1]) \\ P[i,j+1] = P[i,j] - \Delta P_{annular}[i,j] \end{cases} \tag{22}$$

By assuming a column wall temperature equal to the surrounding rock temperature ($T_w[i,j] = T_{hot}[i]$), the elementary heat transfer coefficients U[i,j] are computed using the local Nusselt number correlation recommended by Jackson [31] for the forced convection case along a vertical turbulent flow of supercritical CO_2:

$$Nu[i,j] = 0.0183\, Re^{0.82}[i,j] Pr^{0.5}[i,j] \left(\frac{\rho[i,j]}{\rho_w[i,j]}\right)^{-0.3} \tag{23}$$

4.2. Results and discussion: ΔT_{min} impact

Coupling the thermodynamic model of the storage system described in Section 2 and the hot reservoir heat exchanger model described in Section 4.1 gives the results illustrated in Figs. 9a and b, with reference to the regenerative basic system and 1 MW_{el} power output; the cold storage temperature T_{cold} and the operating pressures being optimal. The figures show that the number of columns, the overall pressure drop (P'_3–P'_4) and the roundtrip efficiency η_{sys} are all sensitive to the minimum temperature difference ΔT_{min} setting. By analysing the (2 series/MW_{el}) case, a ΔT_{min} located between 5 and 8 K could be a good compromise between these three variants. Nevertheless, the overall pressure drop remains significant and contributes to the degradation of the roundtrip efficiency. On the other hand, the addition of series of columns to (4 series/MW_{el}) allows to further reduce the pressure drop and then to improve the roundtrip efficiency. However, it is obvious that this is at the expense of the number of drillings and columns. Here, the choice could be submitted to technical and eco-

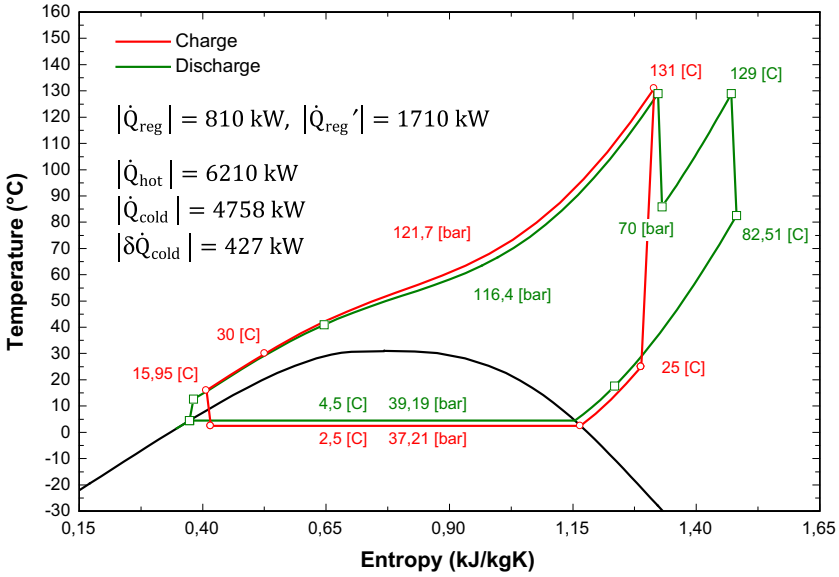

Fig. 7. Entropy diagram of a regenerative advanced system including a two-phase turbine in the charging cycle and a two-stage discharging cycle (ΔT_{min} = 1 K, $\dot{W}_{el}'$ = 1 MW_{el}, η_{sys} = 65%).

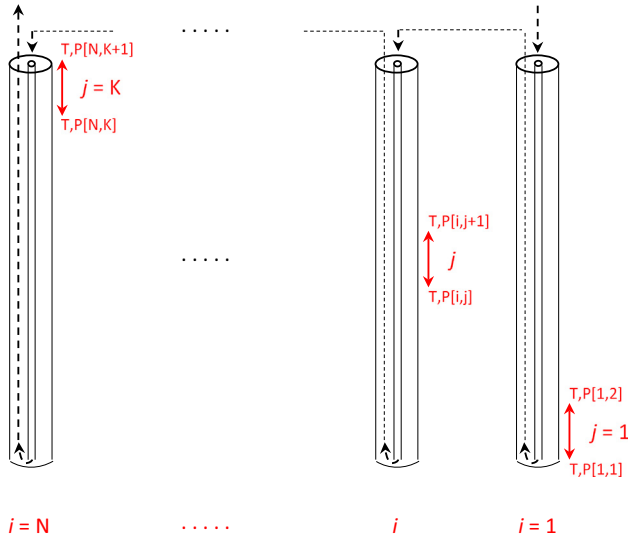

Fig. 8. Conceptual scheme of a one series discretization.

Table 2
Column geometry.

Column length	15.3 m
Central tube length	15 m
Column internal diameter	0.4 m
Central tube internal diameter	0.2 m

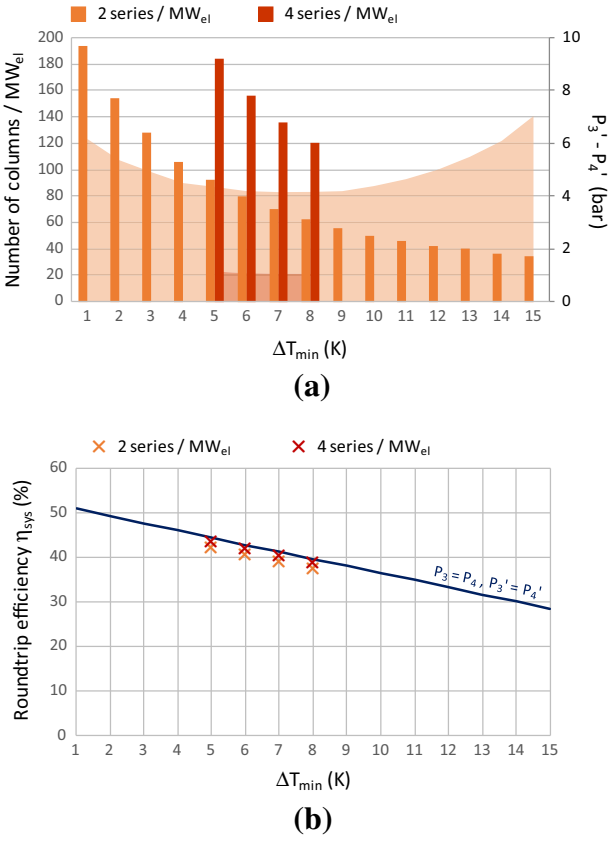

Fig. 9. ΔT_{min} impact on: (a) number of columns and pressure drop, (b) roundtrip efficiency.

nomic criteria which are typically depending on the targeted power output. Furthermore, the review and the optimization of the geometric configuration of the unitary column might also be decisive.

By considering the hot reservoir heat exchanger constraints, Table 3 gathers the nominal operations and performances of the various system designs, with reference to ΔT_{min} = 5 K and 1 MW_{el} power output. By comparing the assessed performances with the highest ones given in Section 3 for ΔT_{min} = 1 K and zero pressure losses, the decrease in roundtrip efficiency is nearly the same for the various system design and is around [13–19%] depending on the column number.

The regenerative basic system would finally lead to moderate efficiencies at nominal conditions:

Table 3
TEES systems: operations and performances (ΔT_{min} = 5 K, 1 MW_{el} power output).

Thermo-Electric Storage System				System 1		System 2		System 3	
				Regenerative basic system		Two-stage discharge		Two-phase turbine Two-stage discharge	
Hot reservoir heat exchanger	Number of series			2	4	2	3	2	3
	Total column number			92	184	120	180	120	180
	Re[a]	Central injection tube		10^6 – 4 10^6	7 10^5 – 2 10^6	2 10^6 – 5 10^6	10^6 – 3 10^6	2 10^6 – 5 10^6	10^6 – 3 10^6
		Annular		5 10^5 – 2 10^6	2 10^5 – 7 10^5	6 10^5 – 2 10^6	4 10^5 – 10^6	6 10^5 – 2 10^6	4 10^5 – 10^6
	U (W/m^2K)[a]		HP	326 – 683	186 – 388	324 – 580	233 – 417	352 – 570	253 – 409
			LP	-	-	279 – 302	202 – 217	299 – 331	216 – 237
	ΔP (bar)[a]		HP	4.4	1.1	3.2	1.4	3.2	1.4
			LP	-	-	3.4	1.5	3.4	1.5
Charging process	Mass flow rate (kg/s)		$\dot{m}$ (kg/s)	29.37	28.58	28.16	26.98	29.11	27.97
	Thermodynamic states P (bar) / T (°C) h (kJ/kg)		1	35.2 / 0.4 317.8	35.2 / 0.4 317.8	39.5 / 4.8 314.8	39.5 / 4.8 314.8	42.8 / 8 312	42.8 / 8 312
			2	35.2 / 25 354.5	35.2 / 25 354.5	39.5 / 25 348.2	39.5 / 25 348.2	42.8 / 25 342.8	42.8 / 25 342.8
			3	119.8 / 135 428.6	119.8 / 135 428.6	134.8 / 135 420	134.8 / 135 420	147.1 / 135 413	147.1 / 135 413
			4	115.8 / 30 153.7	118.8 / 30 153	131 / 30 150.3	133.1 / 30 149.9	143 / 30 148.2	145.3 / 30 147.9
			5	115.8 / 15.7 117	118.8 / 15.5 116.3	131 / 16.2 116.9	133.1 / 16.1 116.5	143 / 16.8 117.4	145.3 / 16.8 117.1
			6	35.2 / 0.4 117	35.2 / 0.4 116.3	39.5 / 4.8 116.9	39.5 / 4.8 116.5	42.8 / 8 109.1	42.8 / 8 108.6
	External heat fluxes		$\lvert\dot{Q}_{hot}\rvert$ (kW)	8075	7878	7592	7285	7706	7413
			$\dot{Q}_{cold}$ (kW)	5896	5758	5570	5347	5907	5690
	Internal heat flux		$\lvert\dot{Q}_{reg}\rvert$ (kW)	1078	1049	941	901	897	862
	Compressor power		$\dot{W}_c$ (kW)	2179	2120	2022	1938	2042	1962
	TP turbine power		$\lvert\dot{W}_{tp}\rvert$ (kW)	-	-	-	-	243	239
	Net power input		$\dot{W}_{el}$ (kW_{el})	2223	2163	2063	1977	1835	1758
	COP_{hot}			3.6	3.6	3.7	3.7	4.2	4.2
	COP_{cold}			2.6	2.6	2.7	2.7	3.2	3.2
Discharging process	Mass flow rate (kg/s)		$\dot{m}'$ (kg/s)	31.65	30.77	30.94	29.49	32.63	31.2
	Thermodynamic states P (bar) / T (°C) h (kJ/kg)		1	45.5 / 10.4 113.7	45.5 / 10.4 113.7	50.6 / 14.8 126.2	50.6 / 14.8 126.2	54.7 / 18 136.1	54.7 / 18 136.1
			2	119.5 / 18.9 124.5	119.5 / 18.9 124.5	134.5 / 25.7 138.9	134.5 / 25.7 138.9	146.8 / 31.1 150.4	146.8 / 31.1 150.4
			3	114.5 / 33.8 165.3	114.5 / 32.8 162.3	129.5 / 49.2 210.4	129.5 / 49.2 210.4	141.8 / 53 215.3	141.8 / 53 215.3
			4 HP	110.1 / 125 420.4	113.4 / 125 418.4	126.3 / 125 410.2	128.1 / 125 409.1	138.6 / 125 402.4	140.4 / 125 401.3
			5 HP	45.5 / 53.1 377.4	45.5 / 50.7 374.4	86.6 / 92.7 391.5	84.7 / 89.6 388.7	93.8 / 91.6 383.6	91.9 / 88.8 381
			4 LP	-	-	83.2 / 125 437	83.2 / 125 437	90.4 / 125 432.7	90.4 / 125 432.7
			5 LP	-	-	50.6 / 84.2 410.1	50.6 / 84.2 410.1	54.7 / 83.4 405.9	54.7 / 83.4 405.9
			6	45.5 / 23.9 336.6	45.5 / 23.9 336.6	50.6 / 30.7 338.6	50.6 / 30.7 338.6	54.7 / 36.1 341	54.7 / 36.1 341
	External heat fluxes		$\dot{Q}'_{hot}$ (kW)	8075	7878	7592	7285	7706	7413
			$\lvert\dot{Q}'_{cold}\rvert$ (kW)	7054	6858	6572	6265	6686	6393
	Internal heat flux		$\lvert\dot{Q}'_{reg}\rvert$ (kW)	1292	1164	2213	2109	2118	2026
	Feed pump		$\dot{W}'_p$ (kW)	341	333	392	374	467	447
	Turbine power	HP	$\lvert\dot{W}'_{t1}\rvert$ (kW)	1362	1353	579	600	613	631
		LP	$\lvert\dot{W}'_{t2}\rvert$ (kW)	-	-	833	794	874	836
	Net power output		$\lvert\dot{W}'_{el}\rvert$ (kW_{el})	1000	1000	1000	1000	1000	1000
	Thermal efficiency		η_{th} (%)	12.4	12.7	13.2	13.7	13	13.5
Chiller	Chiller heat flux		$\lvert\delta\dot{Q}_{cold}\rvert$ (kW)	1158	1100	1002	918	779	703
	Chiller power input		$\dot{W}''_{el}$ (kW_{el})	112	106	67	61	38	34
	COP			10.3	10.4	15	15	20.5	20.6
Roundtrip efficiency			η_{sys} (%)	42.8	44.1	46.9	49	53.4	55.8

[a] Values related to the discharging process.

- $\eta_{sys} \approx 44\%$ with a ground exchanger of around 1800 columns for a 10 MW_{el} power output
- $\eta_{sys} \approx 42.5\%$ with a ground exchanger of around 1000 columns for a 10 MW_{el} power output.

A regenerative system including a two-stage discharging cycle would lead at nominal conditions to:

- $\eta_{sys} \approx 49\%$ with a ground exchanger of around 1800 columns for a 10 MW_{el} power output
- $\eta_{sys} \approx 47\%$ with a ground exchanger of around 1200 columns for a 10 MW_{el} power output.

A regenerative advanced system including a two-phase turbine in the charging cycle and a two-stage discharging cycle would lead at nominal conditions to:

- $\eta_{sys} \approx 55.5\%$ with a ground exchanger of around 1800 columns for a 10 MW_{el} power output
- $\eta_{sys} \approx 53.5\%$ with a ground exchanger of around 1200 columns for a 10 MW_{el} power output.

5. Conclusion

The work presented in this paper deals with a new concept of thermo-electric energy storage system combining CO_2 transcritical cycles and ground heat storage. The conceptual design of such TEES system is addressed only from a thermodynamic point of view and the assessment is limited, as a first approach, to the nominal-operation charging/discharging time.

In the first part of the work, various system designs are assessed and compared basing on the maximum reachable roundtrip efficiencies where the ground exchanger constraints are first side-stepped (ΔT_{min} = 1 K, zero pressure losses). The main results have shown roundtrip efficiencies up to 50%, able to reach 66% with the most complex system. This part has also emphasized the importance to provide heat regeneration in both charging and discharging processes. This double regeneration appears very attractive to meet high efficiency and low investment cost. It is particularly significant when considering a multi-stage discharging process.

In the second part of the work, a one-dimensional model of the multicolumn ground exchanger is performed and coupled to the thermodynamic model of the storage system. This model coupling has indicated that the number of drillings and columns, the overall pressure drop and the roundtrip efficiency are all sensitive to the minimum temperature difference ΔT_{min} setting. The results have also shown that a ΔT_{min} located between 5 and 8 K could be a good compromise between these three variants. Also, the addition of series of columns in a serial-parallel arrangement allows to further reduce the exchanger pressure losses and then to improve the roundtrip efficiency. This part has revealed roundtrip efficiencies from 42.5 to 55.5% with a ΔT_{min} of 5 K.

This steady-state simulation is *in fine* important to introduce the new concept, to give a comparative analysis for the selection of the system design and to provide a preliminarily design of the ground exchanger according to the system design and the net power output. Further work through the SELECO2 project would include turbomachinery modelling and transient simulation so that it will be possible to (i) study the heat transfer evolution during the off-design condition times (ii) better understand the dependency between the charging and the discharging processes and (iii) gather for each process the nominal-condition time and the off-design condition times in the calculation of the roundtrip efficiency of the storage system. This would lead to a complete overview of the new concept and a better evaluation of the general interest.

Acknowledgement

The authors acknowledge the support of the French Research National Agency (ANR) under grant ANR-13-SEED-0004 (SELECO2 project) and the contribution of all partners of the project (ENGIE, Toulouse University, BRGM, CEA, ENERTIME).

References

[1] ENEA Consulting, Facts & Figures: Le Stockage d'Energie, 2012.
[2] T. Fujihara, H. Imano, K. Oshima, Development of pump turbine for seawater pumped-storage power plant, Hitachi Rev. 47 (5) (1998) 199–202.
[3] F. Crotogino, K.-U. Mohmeyer, R. Scharf, Huntorf CAES: more than 20 years of successful operation, in: Proc of SMRI Spring Meeting, Orlando, Florida, USA, 2001.
[4] PowerSouth Energy Cooperative, CAES McIntosh Alabama.
[5] Chris Bullough, Christoph Gatzen, Christoph Jakiel, Martin Koller, Andreas Nowi, Stefan Zunft, Advanced adiabatic compressed air energy storage for the integration of wind energy, in: Proceedings of the European Wind Energy Conference, London UK, 2004.
[6] G. Grazzini, A. Milazzo, Thermodynamic analysis of CAES/TES systems for renewable energy plants, Renew. Energy 32 (2008) 1998–2006.
[7] M. Mercangöz, J. Hemrle, L. Kaufmann, A. Z'Graggen, C. Ohler, Electrothermal energy storage with transcritical CO_2 cycles, Energy 45 (2012) 407–415.
[8] M. Mercangoez, J. Hemrle, L. Kaufmann, Thermoelectric energy storage system having two thermal baths and method for storing thermoelectric energy. Patent EP2241737.
[9] C. Ohler, M. Mercangoez, Thermoelectric energy storage system and method for storing thermoelectric energy. Patent EP2182179.
[10] M. Morandin, F. Maréchal, M. Mercangöz, F. Buchter, Conceptual design of a thermo-electrical energy storage system based on heat integration of thermodynamic cycles, Energy 45 (2012) 375–396.
[11] M. Morandin, M. Mercangöz, J. Hemrle, F. Maréchal, D. Favrat, Thermoeconomic design optimization of a thermo-electric energy storage system based on transcritical CO_2 cycles, Energy 58 (2013) 571–587.
[12] T. Desrues, J. Ruer, P. Marty, J.F. Fourmigué, A thermal energy storage process for large scale electric applications, Appl. Therm. Eng. 30 (5) (2010) 425–432.
[13] S. Henchoz, F. Buchter, D. Favrat, M. Morandin, M. Mercangoez, Thermoeconomic analysis of a solar enhanced energy storage concept based on thermodynamic cycles, Energy 45 (1) (2012) 358–365.
[14] Y.M. Kim, D.G. Shin, S.Y. Lee, D. Favrat, Isothermal transcritical CO_2 cycles with TES (thermal energy storage) for electricity storage, Energy 49 (2013) 484–501.
[15] Y.M. Kim, C.G. Kim, D. Favrat, Transcritical or supercritical CO_2 cycles using both low- and high-temperature heat sources, Energy 43 (2012) 402–415.
[16] M. Li, J. Wang, Xurong Wang, W. He, Y. Dai, Thermo-economic analysis and comparison of a CO_2 transcritical power cycle and an organic Rankine cycle, Geothermics 50 (2014) 101–111.
[17] E. Cayer, N. Galanis, M. Désilets, H. Nesreddine, P. Roy, Analysis of a carbon dioxide transcritical power cycle using a low temperature source, Appl. Energy 86 (2009) 1055–1063.
[18] E. Cayer, N. Galanis, H. Nesreddine, Parametric study and optimization of a transcritical power cycle using a low temperature source, Appl. Energy 87 (2010) 1349–1357.
[19] T. Held, Initial test results of a megawatt-class supercritical CO_2 heat engine, in: The 4th International Symposium – Supercritical CO_2 Power Cycles, 2014. September 9–10; Pittsburgh, USA.
[20] S. Lanini, F. Delaleux, X. Py, R. Olivès, D. Nguyen, Improvement of borehole thermal energy storage design based on experimental and modelling results, Energy Build. 77 (2014) 393–400.
[21] S.A. Klein, Engineering Equation Solver, F-Chart Software, Middleton, WI, 2010.
[22] A. Schuster, S. Karellas, R. Aumann, Efficiency optimization potential in supercritical organic Rankine cycles, Energy 35 (2010) 1033–1039.
[23] C. He, C. Liu, H. Gao, H. Xie, Y. Li, S. Wu, J. Xu, The optimal evaporation temperature and working fluids for subcritical organic Rankine cycle, Energy 38 (2012) 136–143.
[24] F. Ayachi, E. Boulawz Ksayer, P. Neveu, Exergy assessment of recovery solutions from dry and moist gas available at medium temperature, Energies 5 (2012) 718–730.
[25] F. Ayachi, E. Boulawz Ksayer, A. Zoughaib, P. Neveu, ORC optimization for medium grade heat recovery, Energy 68 (2014) 47–56.
[26] S. Lecompte, H. Huisseune, M. van den Broek, M. De Paepe, ORC methodical thermodynamic analysis and regression models of organic Rankine cycle architectures for waste heat recovery, Energy 87 (2015) 60–76.
[27] M.H. Yang, R.H. Yeh, Thermodynamic and economic performances optimization of an organic Rankine cycle system utilizing exhaust gas of a large marine diesel engine, Appl. Energy 149 (2015) 1–12.
[28] A. Pezzuolo, A. Benato, A. Stoppato, A. Mirandola, The ORC-PD: a versatile tool for fluid selection and organic Rankine cycle unit design, Energy 102 (2016) 605–620.
[29] A. Landelle, N. Tauveron, P. Haberschill, R. Revellin, S. Colasson, Experimental and analytical study of transcritical organic Rankine cycles at low temperature, in: ASME ORC Conference, 2015.
[30] N. Tauveron, S. Colasson, J.-A. Gruss, Available systems for the conversion of waste heat to electricity, in: ASME-IMECE Conference, 2014.
[31] J.D. Jackson, W.B. Hall, J. Fewster, A. Watson, M.J. Watts, Heat transfer to supercritical fluids, U.K.A.E.A. A.E.R.E.-R. 8158, 1975, Design Report 34.